

## Enhanced second harmonic generation in ferroelectric nematics by doping D- $\pi$ -A chromophores

Runli Xia<sup>a</sup>, Xiuhu Zhao<sup>a</sup>, Jinxing Li<sup>a</sup>, Huanyu Lei<sup>a</sup>, Yaohao Song<sup>a</sup>, Weifeng Peng<sup>a</sup>, Xinxin Zhang<sup>a</sup>, Satoshi Aya<sup>a,b</sup>, Mingjun Huang<sup>a,b</sup>

<sup>1</sup> South China Advanced Institute for Soft Matter Science and Technology (AISMST), School of Emergent Soft Matter, South China University of Technology, Guangzhou 510640, China.

<sup>2</sup> Guangdong Provincial Key Laboratory of Functional and Intelligent Hybrid Materials and Devices, South China University of Technology, Guangzhou 510640, China.

E-mail: satsoshiaya@scut.edu.cn (SA); huangmj25@scut.edu.cn (MH)

### Contents:

1. Methods
2. Synthesis
3. Figures
4. Table

## 1. Methods

**Differential Scanning Calorimetry (DSC).** Thermal properties of all the samples were characterized utilizing a TA Instruments DSC 2500 with an Intercooler 2P apparatus. The temperature and heat flow scales were calibrated at different heating and cooling rates (5-10 °C/min) using a series of standard materials. For each run of the experiments, the initial mass of the samples used was about 3-5 mg under nitrogen flow.

**Density Functional Theory Calculation.** All DFT calculations were performed with the Gaussian 09 series of programs (Gaussian 09, Revision D.01). The DFT method of RCAM-B3LYP/Aug-CC-pVDZ basis set was used.

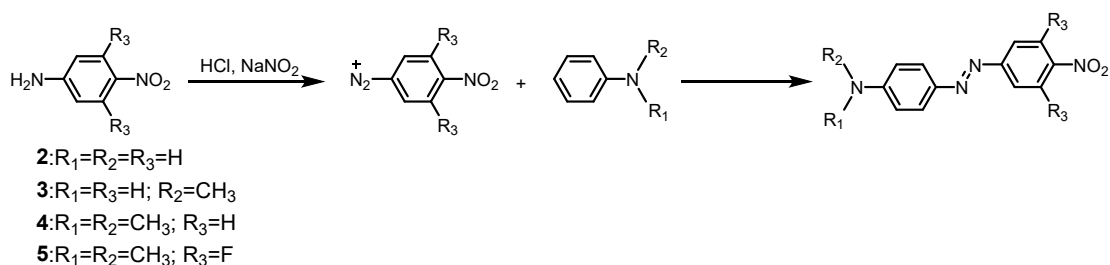
**SHG measurement.** We use a fundamental beam from a Q-switched pulsed laser (MPL-III-1064-20 $\mu$ J) with a central wavelength of 1064 nm, maximum power of 200 mW, pulse duration of 5 ns, and 100 Hz repetition. The fundamental beam is set to be polarized and directed into LC cells. The schematic of the optical system is shown in fig. S9. The SH light is detected in the transmission geometry by a photomultiplier tube (DH-PMT-D100V, Daheng Optics). For the temperature scanning, the SH signal is recorded every 1°C under the control of a homemade Labview program.

### **$d_{33}$ measurement.**

We inject  $N_F$  liquid crystal material into parallel rubbing wedge-cell, and slowly cool down until the material enters the  $N_F$  phase. We use the PD1&KIM001 piezoelectric inertial stage to control the parallel movement of the liquid crystal cell and change the thickness of the  $N_F$  liquid crystal material at the laser pass. We measure the SHG intensity of the material for each parallel movement. Finally, the SHG intensity at different thicknesses is obtained, and the  $d_{33}$  is obtained by fitting the phase mismatch theory.

## 2. Synthesis

**Dyes 2-4** have been previously reported in the literature (Refs 38-41), and **dye 5** is a new material designed by us. The general synthesis method is shown below:



Nitroaniline (1 eq), HCl (5 eq), and H<sub>2</sub>O (100 eq) were added to the flask and heated with stirring until the reactants were completely dissolved. After 20 min, the diazotized nitroaniline suspension was cooled to around 0°C. Aniline (1 eq) was dissolved in an iced dilute HCl (10%) solution and added to the suspension above with vigorous stirring. Neutralize the mixture to pH=7 with NaOH (10%) solution. The brown-red (**dyes 2**、**3**、**5**) and purple (**dye 4**) powders were filtered out. The products were isolated from the crude mixture by column chromatography over silica with ethyl acetate and petroleum ether as the eluent.

### **4-((4-nitrophenyl)diazenyl)aniline (2)**<sup>38</sup>

<sup>1</sup>H NMR (500 MHz, DMSO-d<sub>6</sub>) δ 8.44 – 8.18 (m, 2H), 7.99 – 7.81 (m, 2H), 7.78 – 7.60 (m, 2H), 6.77 – 6.60 (m, 2H), 6.48 (s, 2H). <sup>13</sup>C NMR (126 MHz, DMSO-d<sub>6</sub>) δ 156.84, 155.05, 147.31, 143.63, 127.05, 125.51, 122.93, 114.10.

### **N-methyl-4-((4-nitrophenyl)diazenyl)aniline (3)**<sup>39</sup>

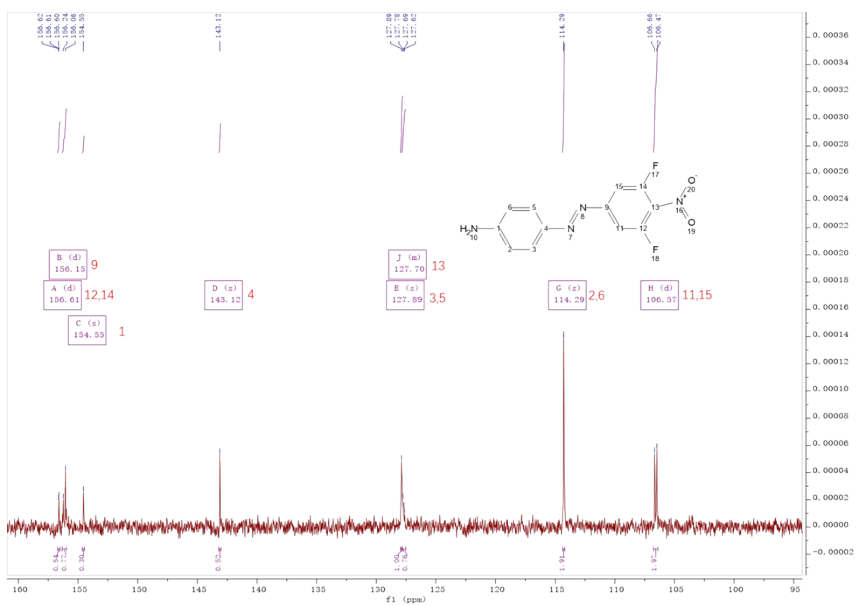
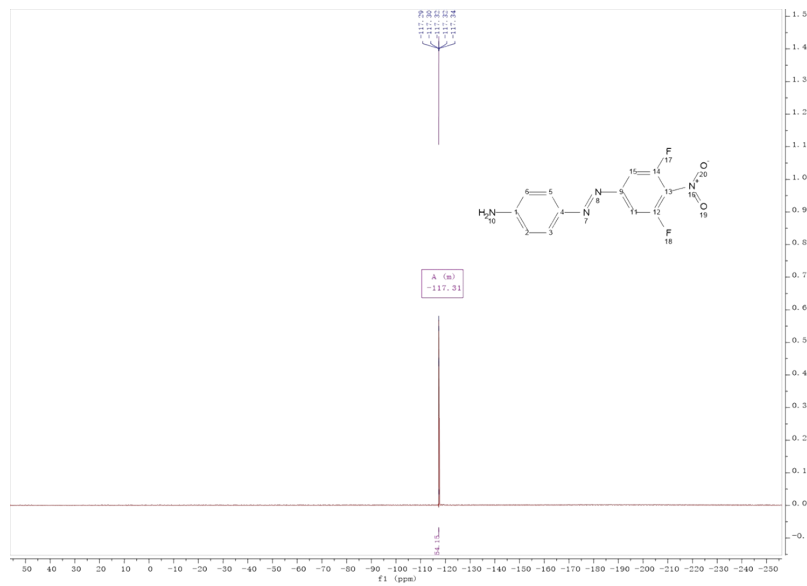
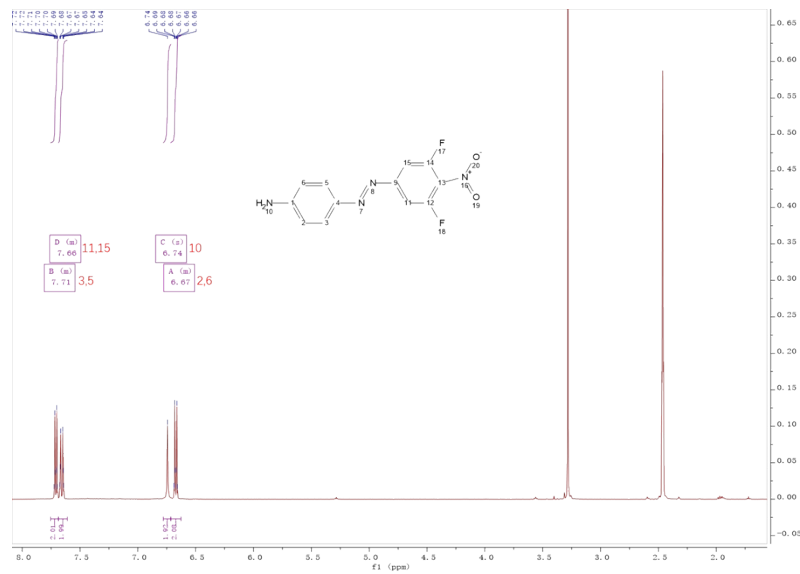
<sup>1</sup>H NMR (500 MHz, DMSO-d<sub>6</sub>) δ 8.34 – 8.29 (m, 2H), 7.91 – 7.85 (m, 2H), 7.79 – 7.74 (m, 2H), 7.10 (s, 1H), 6.70 – 6.61 (m, 2H), 2.79 (d, J = 3.2 Hz, 3H). <sup>13</sup>C NMR (126 MHz, DMSO-d<sub>6</sub>) δ 156.86, 154.90, 147.27, 143.63, 126.95, 125.51, 122.92, 112.15, 29.83.

### **N,N-dimethyl-4-((4-nitrophenyl)diazenyl)aniline (4)**<sup>40</sup>

<sup>1</sup>H NMR (500 MHz, Chloroform-d) δ 8.35 – 8.29 (m, 2H), 8.04 – 7.90 (m, 4H), 6.84 – 6.75 (m, 2H), 3.16 (s, 6H). <sup>13</sup>C NMR (126 MHz, DMSO-d<sub>6</sub>) δ 156.77, 154.07, 147.42, 143.36, 126.43, 125.54, 123.04, 112.26, 29.39 (d, J = 32.7 Hz).

### **(E)-4-((3,5-difluoro-4-nitrophenyl)diazenyl)aniline (5)**

<sup>1</sup>H NMR (500 MHz, DMSO-d<sub>6</sub>) δ 7.74 – 7.69 (m, 2H), 7.68 – 7.62 (m, 2H), 6.74 (s, 2H), 6.70 – 6.64 (m, 2H). <sup>19</sup>F NMR (471 MHz, DMSO-d<sub>6</sub>) δ -117.26 – -117.33 (m). <sup>13</sup>C NMR (126 MHz, DMSO-d<sub>6</sub>) δ 156.62, 156.15 (d, J = 22.7 Hz), 154.55, 143.12, 127.89, 127.88 – 127.53 (m), 114.29, 106.57 (d, J = 23.9 Hz). MS: M+H<sup>+</sup>, 279.0689 (calculated 279.06)



**<sup>1</sup>H NMR, <sup>19</sup>F NMR and <sup>13</sup>C NMR of dye 5**

### 3. Figures

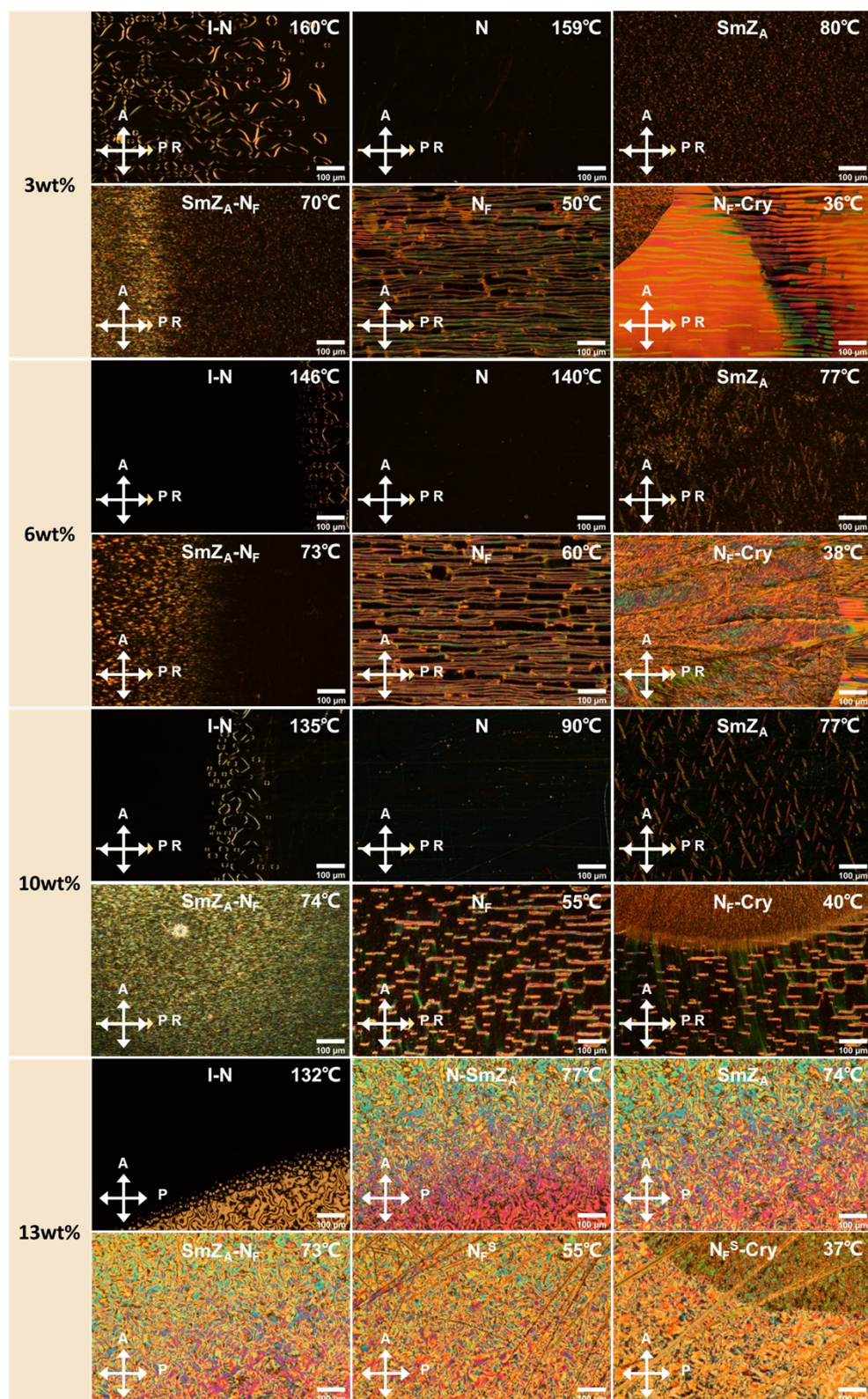


**Fig. S1.** The representative PLM texture evolution of 1/DIO mixtures under crossed polarizers in an LC cell with planar alignment. Yellow arrow: parallel rubbing alignment in substrates. The superscript "S" on phase identification indicates the occurrence of phase separation. Cell thickness: 5 μm.

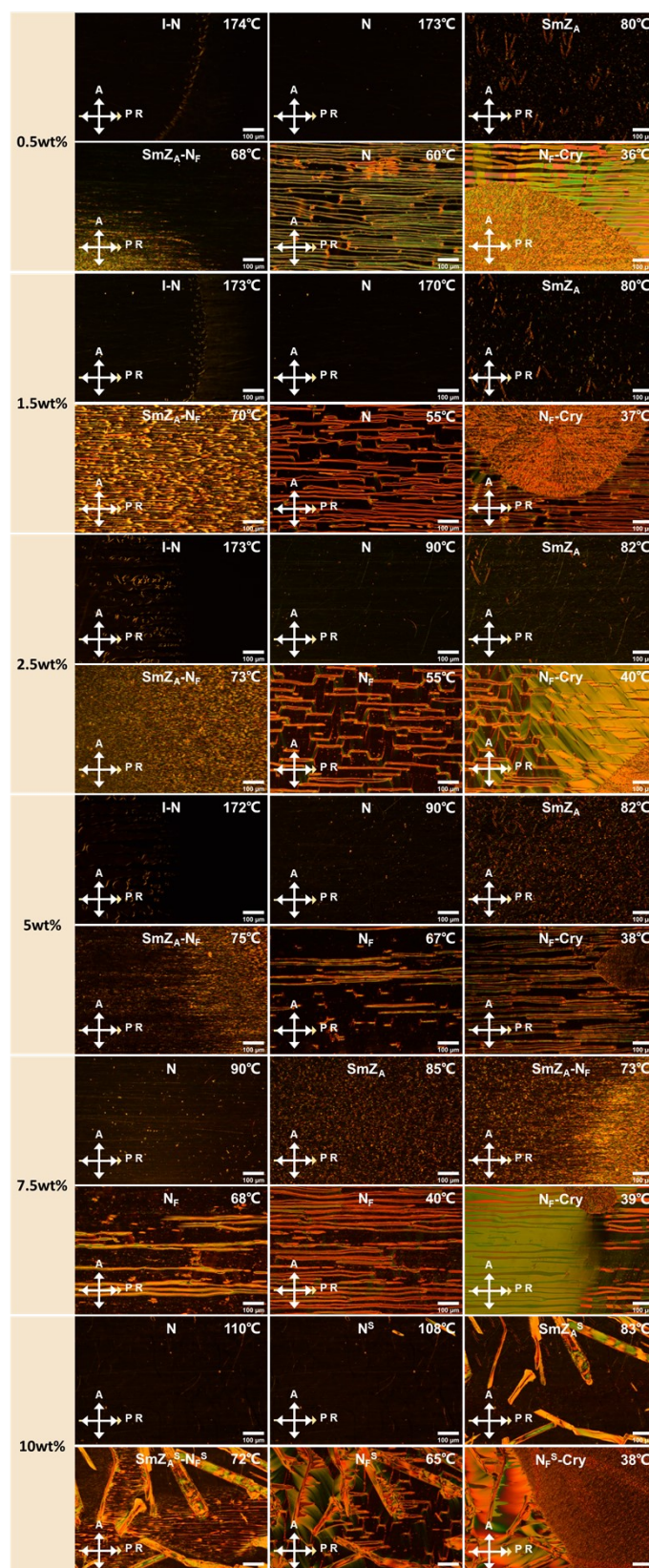


**Fig. S2.** The representative PLM texture evolution of **2/DIO** mixtures under crossed polarizers in an LC cell with planar alignment. Yellow arrow: parallel rubbing alignment in substrates. The superscript “S” on phase identification indicates the occurrence of phase separation. Cell thickness: 5  $\mu\text{m}$ .

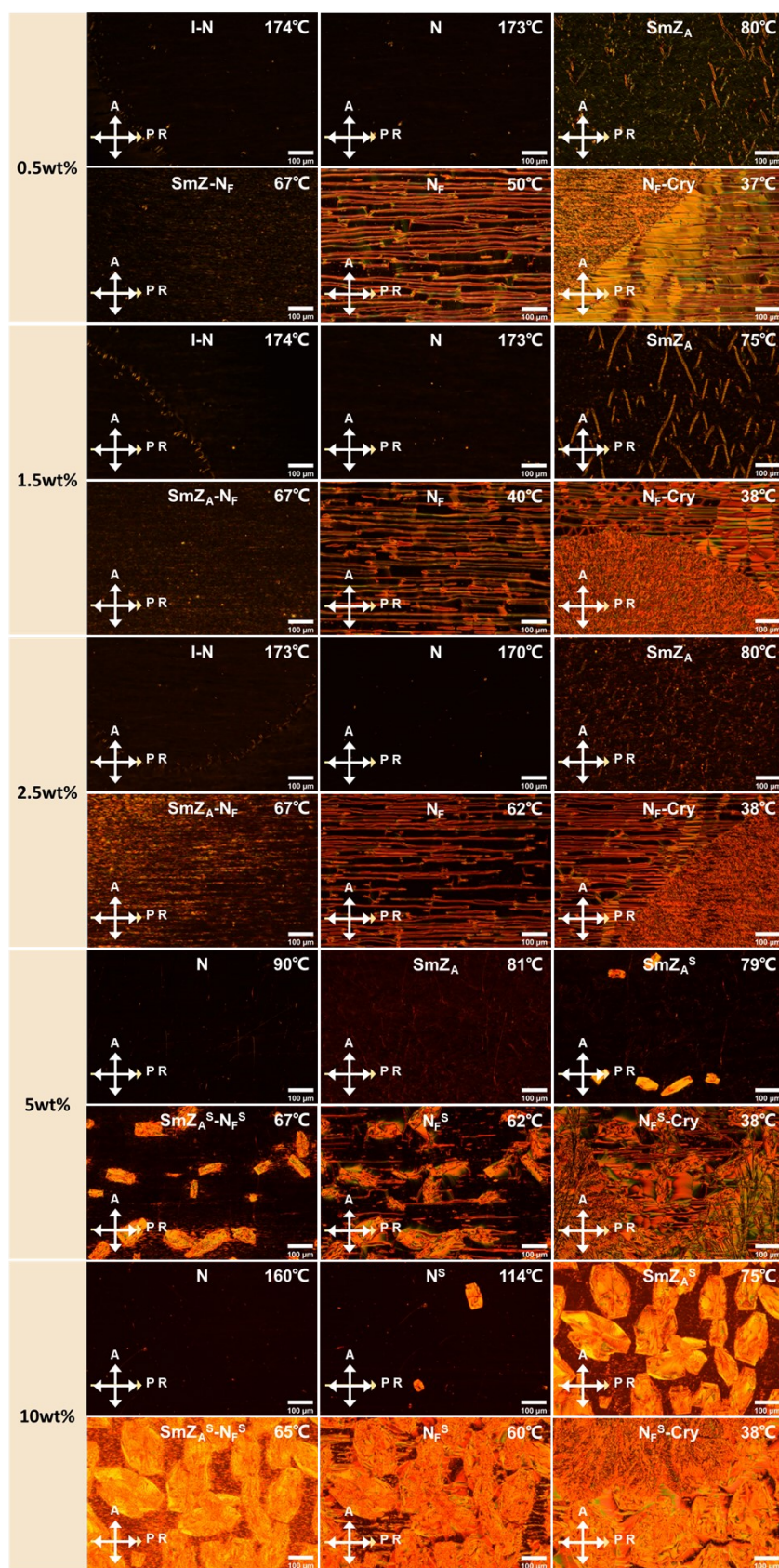


**Fig. S3.** The representative PLM texture evolution of **3/DIO** mixtures under crossed polarizers in an LC cell with planar alignment. Yellow arrow: parallel rubbing alignment in substrates. The superscript S indicates the occurrence of phase separation. Cell thickness: 5 μm.

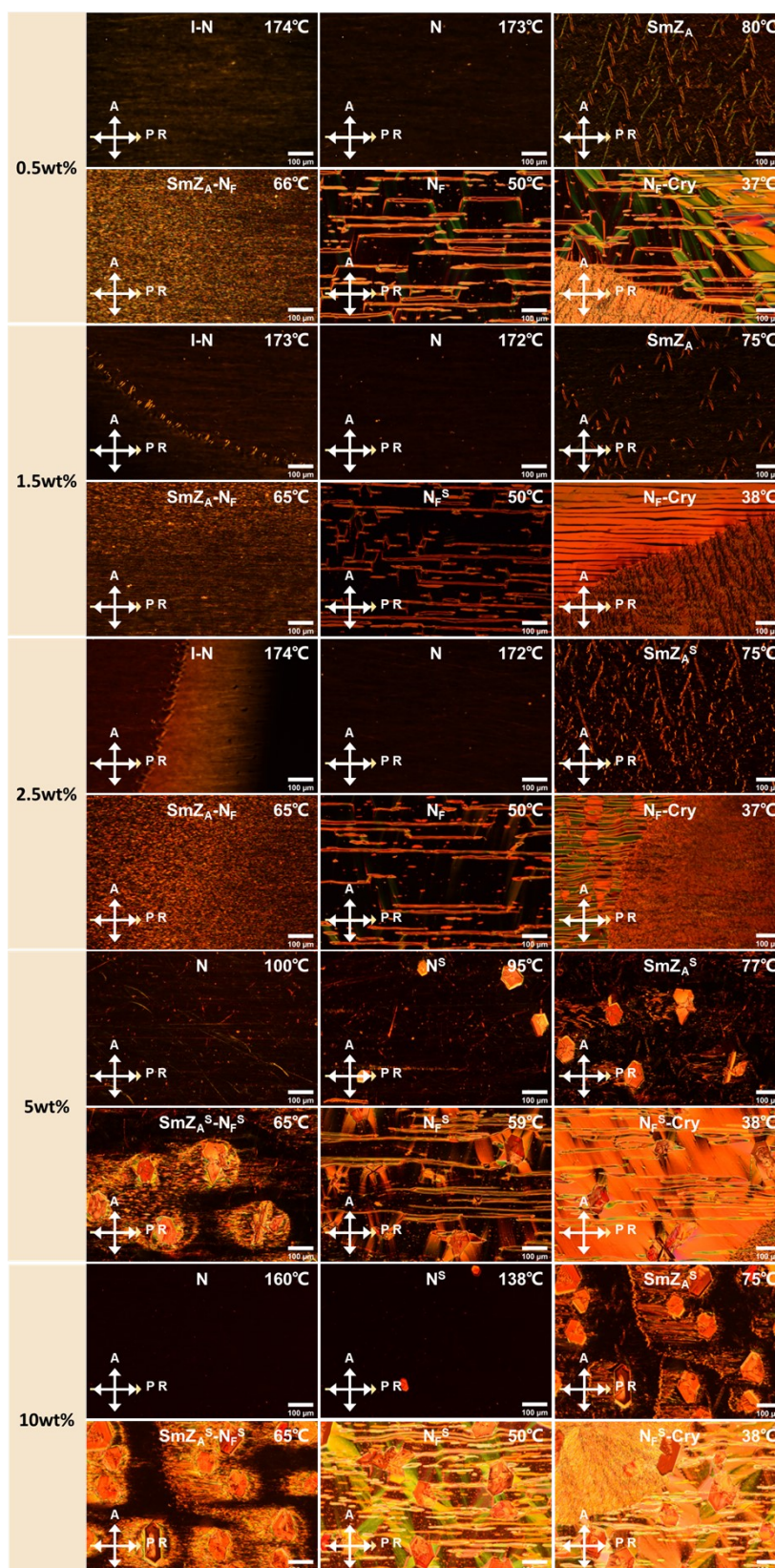


**Fig. S4.** The representative PLM texture evolution of **4/DIO** mixtures under crossed polarizers in an LC cell with planar alignment. Yellow arrow: parallel rubbing alignment in substrates. The superscript "S" on phase identification indicates the occurrence of phase separation. Cell thickness: 5  $\mu\text{m}$ .



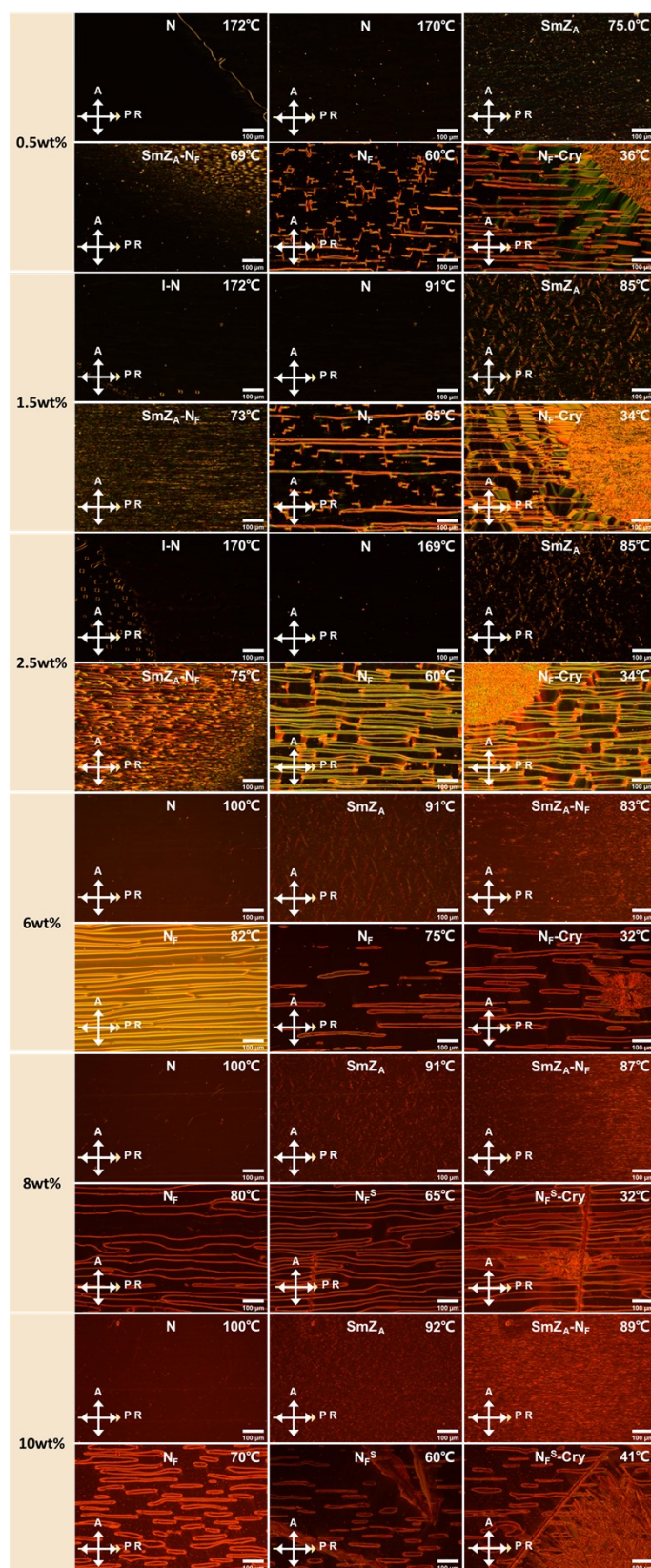


**Fig. S5.** The representative PLM texture evolution of 5/DIO mixtures under crossed polarizers in an LC cell with planar alignment. Yellow arrow: parallel rubbing alignment in substrates. The superscript "S" on phase identification indicates the occurrence of phase separation. Cell thickness: 5  $\mu\text{m}$ .

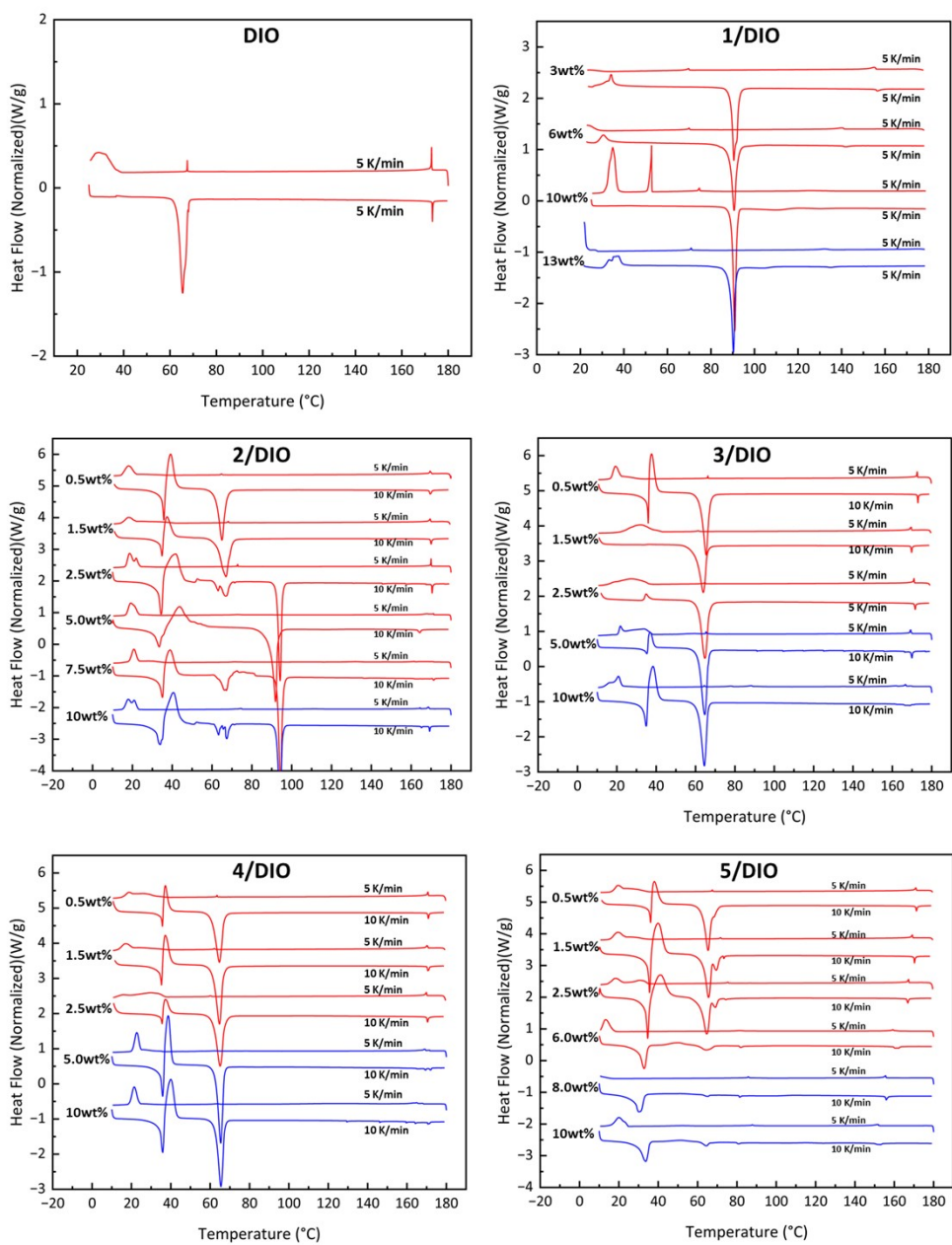


**Fig. S6.** DSC profiles (top: first cooling; bottom: second heating; red: homogeneous system; Blue: heterogeneous system and no-N<sub>F</sub> system) of 1-5/DIO doping systems.

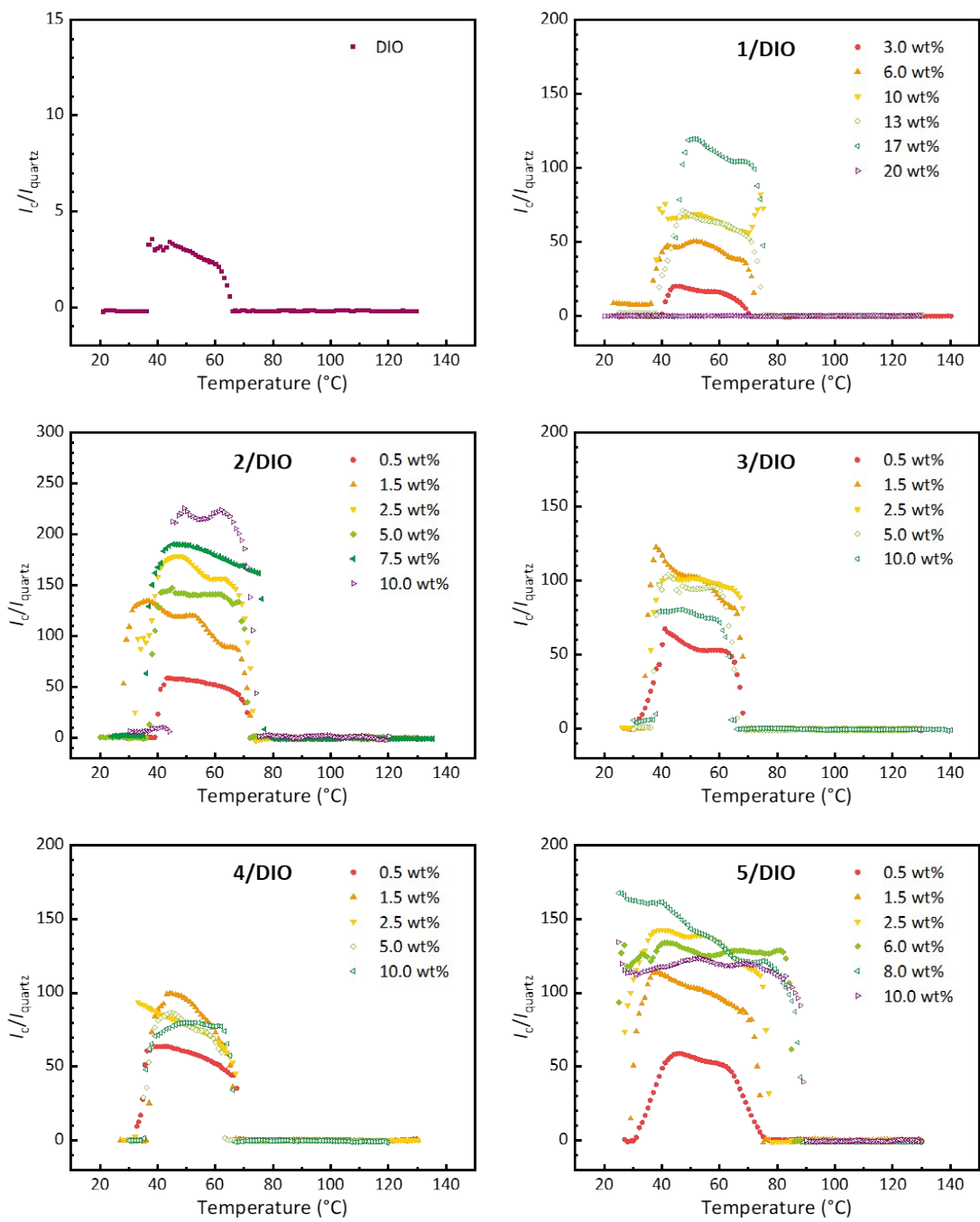


**Fig. S7.** The temperature dependence of SHG intensity of **1-5/DIO** doping systems. Hollow dots mean that phase separation occurs in the system

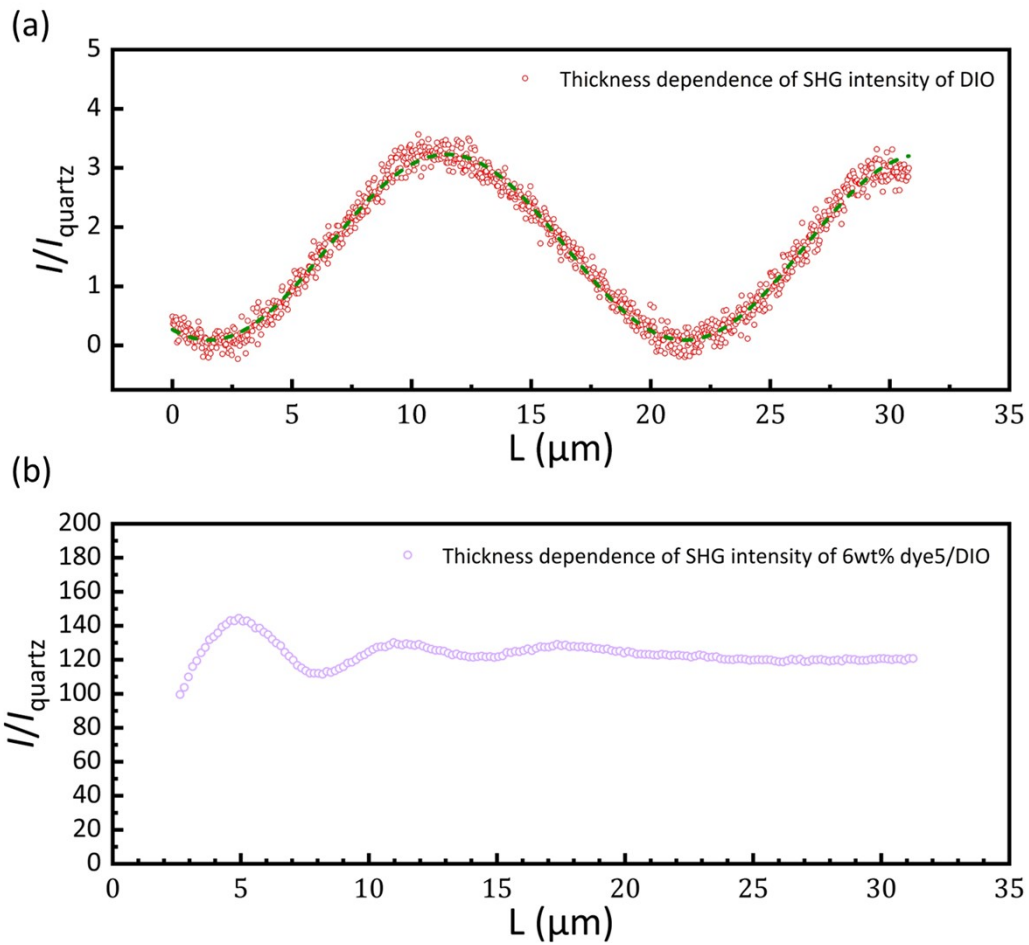


**Fig. S8.** shows the SHG intensity as a function of the thickness  $L$  for **DIO** at  $60\text{ }^{\circ}\text{C}$  (a) and **6wt% dye 5/DIO** at  $78\text{ }^{\circ}\text{C}$  (b). Green dotted line in (a) is a fit to  $A \sin^2 \left[ \frac{2\pi}{\lambda} \Delta n_d L \right]$ , from which  $\Delta n_d = 0.0267$  results. The coefficient  $d_{33}$  was determined from the amplitude  $A$  and resulted to be  $d_{33} = 0.24$  Pm/V for **DIO** at  $60\text{ }^{\circ}\text{C}$ . For **6wt% dye 5/DIO** system, the SHG intensity is no longer sensitive to the phase factor  $\left[ \sin^2 \left[ \frac{2\pi}{\lambda} \Delta n_d L \right] \right]$  as the thickness increases. The amplitude  $A$  of SHG intensity fluctuations gradually decays. And finally, SHG reaches a stable value. The reason for this phenomenon is the presence of a large absorption of the SHG (at a wavelength of 532 nm) by the dye. Nevertheless, the periodicity and maximum value of SHG intensity are still clearly visible, and we thus obtained that  $\Delta n_d = 0.079$ , and  $d_{33} = 4.9$  Pm/V for **6wt% dye 5/DIO** at  $78\text{ }^{\circ}\text{C}$ . The  $\Delta n_d$  of the **dye 5/DIO** is greatly increased compared to that of pure **DIO**, which is caused by the increase of the refractive index  $n$  at 532 nm due to absorption of dye 5.

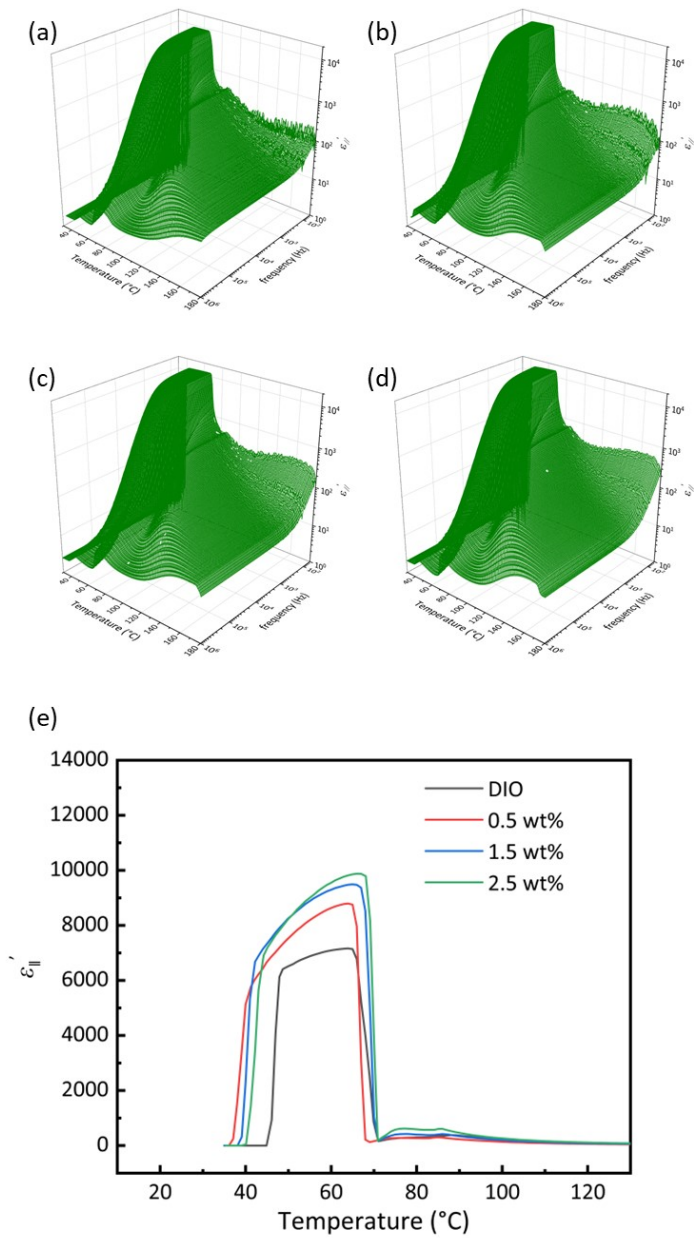


**Fig. S9.** Temperature and frequency dependences of the real part of  $\epsilon_{//}$  (effective) for DIO (a), dye 2/DIO of  $c=0.5$  wt% (b),  $c=1.5$  wt% (c) and  $c=2.5$  wt% (d). The measurements were made at 50 mV<sub>pp</sub>. (e)  $\epsilon_{//}$  (effective) at 1000 Hz.

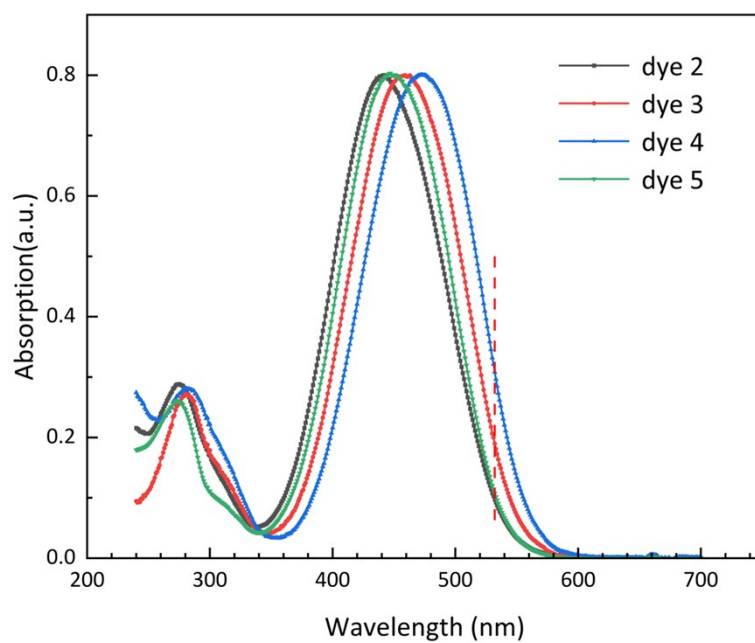


**Fig. S10.** Absorption spectra of dyes **2-5** (measured in THF). Red dotted line:  $\lambda=532$  nm (the wavelength of SH light).

#### 4. Table

<b>NO.</b>	<b>Melting Point (°C)</b>
Dye 1	147
Dye 2	216
Dye 3	202
Dye 4	229
Dye 5	188

**Table S1.** Melting point of the dye molecules. These data are obtained from the DSC test.